Effect of Thickness on the Unsteady Aerodynamics of Closely Coupled Oscillating Airfoils

K. Rokhsaz,* B. P. Selberg,† and W. Eversman‡
University of Missouri-Rolla, Rolla, Missouri 65401

A vortex panel method is presented for the solution of incompressible unsteady aerodynamic problems for airfoils with finite thickness. The accuracy and robustness of the method is demonstrated through comparisons with the existing numerical data and independent test cases. Also, through numerous examples, the flexibility of this method in handling different types of trailing-edge shapes and multiple interfering geometries is shown. Furthermore, the method is used to analyze the effects of airfoil thickness on aerodynamic coefficients of multielement or multiple airfoils. It is shown that, although the influence of thickness is negligible for single element airfoils, it can be profound for closely coupled airfoils and slotted flaps.

Nomenclature

C = reference chord length
$C_{l\alpha}$ = lift coefficient per angle of attack
$C_{m\alpha}$ = pitching moment coefficient per angle of attack
C_p = pressure coefficient
$\bar{D}$ = decalage angle
$\boldsymbol{e}_s$ = unit vector parallel to the surface
$\bar{G}$ = nondimensional gap
h = displacement in plunge
$\boldsymbol{n}$ = unit vector normal to the surface
p = pressure
$\boldsymbol{r}$ = radius vector
S = hypersurface defining the airfoil
$\bar{S}$ = nondimensional stagger
s = coordinate parallel to the surface or the wake
t = time
V = velocity
α = angle of attack
$\bar{\alpha}$ = steady-state angle of attack
α_0 = amplitude of the unsteady angle of attack
γ = local unsteady vorticity
$\bar{\gamma}$ = amplitude of local vorticity
Δ = difference between upper and lower sides
∇ = gradient operator
∇^2 = Laplacian operator
θ = potential of a unit vortex
ξ = coordinate tangent to the wake
ρ = air density
Φ = total velocity potential
ϕ = perturbation velocity potential
ψ = amplitude of unsteady perturbation potential
ω = circular frequency
$\bar{\omega}$ = reduced frequency, $= C\omega/2V_\infty$ (k in aeroelasticity)

Subscripts
i = amplitude of the unsteady components
s = steady-state components
u = unsteady components
∞ = freestream quantities

I. Introduction

AIRFOILS undergoing oscillatory motion can demonstrate aerodynamic characteristics that are substantially different from their steady-state behavior. The most profound of these is the phase difference between the motion and the generation of aerodynamic forces and moments. Accurate prediction of these forces and their phase angles is of major importance in flutter analysis where airfoils are assumed to move harmonically with very small amplitudes. Steady-state aerodynamic behavior of closely coupled airfoils in two-dimensional incompressible flow was studied by the authors in Refs. 1 and 2. It was demonstrated that, although the influence of thickness is not very critical in the case of a single airfoil, it can be profound for closely coupled lifting surfaces. The same behavior is expected to be present for harmonically oscillating airfoils. However, the prediction method for the influence of thickness on oscillating coupled airfoils does not exist. The thin airfoil formulations, which are computationally fast, do not account for the effects of thickness, camber, and nonzero mean incidence angles. On the other hand, the current methods capable of doing so appear to be more of a novelty in nature because of their inapplicability. They either require exorbitant amounts of computation time or they include unacceptable numerical instabilities. Both of these characteristics exclude the use of these methods for flutter analysis where multiple solutions have to be performed accurately and rapidly over a wide range of frequencies. Considering these limitations, in order to study the effect of thickness on the flutter speed of closely coupled airfoils, a fast and robust solution method is developed. It is the intention of this paper to demonstrate such a technique and its application to interfering airfoils. Furthermore, it is intended to demonstrate the effects of thickness on the aerodynamic characteristics of closely coupled airfoils.

Analytical solutions for determining the lift and pitching moment coefficients of a harmonically oscillating airfoil date back to that of Theodorsen.[3] His formulation of the problem resembles the thin airfoil theory used in steady-state aerodynamics. The airfoil is replaced by a flat plate at zero mean incidence angle with respect to the upstream flow. Effects of camber, thickness, and nonzero angles of attack are totally ignored in this formulation. The wake is assumed to be a flat vortex sheet with uniform steady-state velocity equal to that of

Presented as Paper 89-1284 at the AIAA/ASME/ASCE/AHS/ASC 30th Structures, Structural Dynamics, and Materials Conference, Mobile, AL, April 3-5, 1989; received July 5, 1989; revision received June 15, 1990; accepted for publication Sept. 11, 1990.

*Lecturer, Department of Mechanical and Aerospace Engineering and Engineering Mechanics. Senior Member AIAA.

†Professor and Associate Chairman, Department of Mechanical and Aerospace Engineering and Engineering Mechanics. Associate Fellow AIAA.

‡Curators' Professor, Department of Mechanical and Aerospace Engineering and Engineering Mechanics. Associate Fellow AIAA.

the upstream flow. Although this method is applicable to single airfoil cases only, it can accommodate a plain flap through the proper application of the boundary conditions. Like all thin airfoil formulations, this technique results in the difference between the pressures over the upper and lower surfaces of the airfoil.

The first analytical technique that included the effects of thickness was developed by Hewsone-Browne.[4] A similar formulation of the problem was also presented by van de Vooren and van de Vel.[5] These approaches make extensive use of conformal mapping and are only applicable to special classes of airfoils that lend themselves to simple transformations. In both previous investigations, a single symmetric airfoil is placed at zero mean incidence angle and is conformally mapped into a circle. The wake is assumed to be a flat vortex sheet emanating from the trailing edge. However, unlike in Ref. 3, the exact steady-state velocity distribution is used over the wake. For these analytical solutions to become mathematically feasible, the airfoil shape must be transformed into a circle in a simple single-step operation. Although the methods of Refs. 4 and 5 result in the exact pressure distribution, they cannot accommodate flaps, camber, general airfoil shapes, or nonzero mean incidence angles. Furthermore, considering the complexity of transformation of multiple airfoils into circles, these approaches appear to be totally inapplicable to interfering lifting surfaces.

Numerical methods used to determine the aerodynamic coefficients of oscillating airfoils are 1) finite difference methods and 2) surface singularity techniques. Finite difference solutions have the advantage of accommodating nonlinearities very easily. In these methods, the problem is formulated in terms of disturbance velocity potential. The governing equations are simply discretized, replacing derivatives by difference forms regardless of the nature of nonlinearities. The resultant algebraic equations are solved using any of a number of iterative techniques. However, interference of the wake surface with the grid system can pose a rather formidable numerical problem. In order to alleviate these problems, adaptive mesh generation has to be employed at the cost of regenerating the entire grid system for each iteration cycle. Furthermore, since the problem is formulated in terms of the disturbance velocity potential, the grid system has to extend far enough into the solution domain for this variable to vanish. At the same time, in order to achieve an accurate pressure distribution, a very large number of points must be employed on the surface of the airfoil. Finite difference techniques thus require very large amounts of computer storage and/or computation time, which can be a very strong drawback to their use for flutter analysis where multiple solutions over a wide range of frequencies are required.

The second group of numerical techniques called surface singularity (boundary element) methods are based on either an acceleration potential or a velocity potential formulation. Using the acceleration potential, the problem is formulated in terms of the difference in pressures of the lower and the upper surfaces through Euler's equation of motion. The resulting integral equation spans over the leading-edge stagnation streamline as well as over the airfoil. However, the integral equation vanishes on the wake in accordance with the Kutta condition. This approach was first introduced by Possio[6] for the fully linearized compressible subsonic problem. Grzedzinski[7] adopted this method for analyzing the interference problem in incompressible flow over biplanes. Both investigators ignored the effect of thickness on the flowfield.

The first set of boundary element formulation including the effects of thickness in the literature is due to Giesing,[8-10] who used a velocity potential formulation. He introduced a nonlinear as well as a linearized formulation. The airfoil is modeled by source singularity panels with linearly varying strength and a constant strength vortex panel. Giesing's methods resemble that of Hess[11] who considered the steady-state problem. In the nonlinear form, the wake is modeled by a collection of discrete vortices convected downstream of the trailing edge over small increments of time. The linearized formulation of the problem is derived from the nonlinear formulation. In this case, the governing matrices are expanded in series with their higher order terms neglected. Both techniques suffer from strong numerical instabilities, especially for airfoils with cusped trailing edges, as discussed by Hess.[12] Furthermore, the nonlinear solution requires exorbitant amounts of computation time for harmonically oscillating airfoils. Since these methods are posed in terms of the velocity potential, they yield the actual pressure distribution on the surfaces. Also, since surface singularity methods do not require a grid system surrounding the airfoils, their application to multiple interfering airfoils is quite simple.

Another surface singularity method has been proposed by Hounjet.[13] Although this method is used to solve the subsonic flow problem, linearized in Mach number, it should be easily applicable to incompressible flow cases as well. This method employs doublet panels of piecewise continuous strength. A similar approach is also employed by Morino.[14] The weakness of Morino's approach lies in the fact that, with doublet panels, the distribution of the velocity potential over the surface has the same interpolation order as that of the doublet strength, as explained by Banerjee and Butterfield.[15] Therefore, piecewise linear distribution of the velocity requires the use of quadratic distribution of doublets. A linear distribution of doublet strength over the surface results in discontinuities in the velocity components at the node points, and, therefore, numerical instabilities can occur with coarse grids. In three-dimensional cases, the pressure relief effect usually reduces the magnitude of these instabilities. In two-dimensional cases, to alleviate this problem, a very large number of panels must be employed to represent the surface, which in turn increases the required computation time.

II. Formulation

The detailed formulation of the flow equation and its associated boundary conditions and constraints is presented in Ref. 16. In the interest of brevity, the steady-state case is omitted in the following.

A. Governing Equation

As demonstrated by Keuthe and Chow,[17] expressing the continuity equation in terms of the velocity potential for an irrotational incompressible flow results in

$$\nabla^2\Phi = 0 \tag{1}$$

Using the linearity of this equation, the velocity potential can be expressed as the sum of three components:

$$\Phi = \phi_\infty + \phi_s + \phi_u \tag{2}$$

none of which has to be small at this point. Here, ϕ_∞ is used to generalize the equations for cases in which the freestream velocity is not parallel to the chord line. This simplifies the introduction of a nonzero mean angle of attack if it is so desired. Substitution of Eq. (2) into Eq. (1), for the unsteady component, results in

$$\nabla^2\phi_u = 0 \tag{3}$$

B. Boundary Conditions

Boundary conditions related to Eq. (1) are

$$\Phi(r \to \infty) = \phi_\infty \tag{4}$$

$$\frac{DS}{Dt} = 0 \tag{5}$$

Introducing Eq. (2) into these equations, using Eq. (4) for the unsteady part, results in

$$\phi_u(r \to \infty) = 0 \tag{6}$$

For the flow tangency condition, we let

$$S = S_s + S_u \tag{7}$$

therefore

$$\frac{DS}{Dt} = \frac{\partial S_u}{\partial t} + V \cdot (\nabla S_s + \nabla S_u) \tag{8}$$

where

$$V = \nabla(\phi_\infty + \phi_s + \phi_u) \tag{9}$$

Dividing Eq. (8) through by the magnitude of the gradient of S

$$\frac{1}{|\nabla S|}\left(\frac{\partial S_u}{\partial t}\right) + V \cdot (n_s + n_u) = 0 \tag{10}$$

Substituting Eq. (9) into Eq. (10) and separating the time-dependent terms, the unsteady flow boundary condition becomes

$$\frac{1}{|\nabla S|}\left(\frac{\partial S_u}{\partial t}\right) + \nabla\phi_u \cdot n_s + (\nabla\phi_\infty + \nabla\phi_s) \cdot n_u + \nabla\phi_u \cdot n_u = 0 \tag{11}$$

C. Pressure Coefficient

For the origin moving with constant speed V_∞ from Bernoulli's equation

$$\frac{\partial\Phi}{\partial t} + \frac{1}{2}\nabla\Phi \cdot \nabla\Phi + \frac{p}{\rho} = \frac{p_\infty}{\rho} + \frac{1}{2}V_\infty^2 \tag{12}$$

Substituting for Φ from Eq. (2) and rearranging the results, the expression for the time-dependent part of the pressure coefficient becomes

$$C_{pu} = -\frac{2}{V_\infty^2}\left[\frac{\partial\phi_u}{\partial t} + (\nabla\phi_\infty + \nabla\phi_s) \cdot \nabla\phi_u + \nabla\phi_u \cdot \nabla\phi_u\right] \tag{13}$$

D. Kutta Condition

At the trailing edge and over the wake surface, the difference in pressure between the upper and lower surfaces must vanish. From Eq. (13), this implies for unsteady-state flow

$$\Delta\left[(\nabla\phi_\infty + \nabla\phi_s + \nabla\phi_u) \cdot \nabla\phi_u + \frac{\partial\phi_u}{\partial t}\right] = 0 \tag{14}$$

E. Harmonic Motion with Small Amplitude

Equations (3), (11), (13), and (14) are as general as possible. These equations are valid for two- and three-dimensional flows, for arbitrary motions of the wing or airfoil, and for large perturbation velocity potentials. However, Eqs. (11), (13), and (14) are nonlinear. Restricting the motion to harmonic motion with small amplitude allows linearization of these equations. We let

$$\phi_u = \psi\alpha_0 e^{i\omega t}, \qquad S_u = S_i\alpha_0 e^{i\omega t}, \qquad n_u = n_i\alpha_0 e^{i\omega t}$$

where α_0 is the small amplitude of motion. Substituting these into Eqs. (3), (11), (13), and (14) and ignoring the higher order terms results in

$$\nabla^2\psi = 0 \tag{15}$$

$$\nabla\psi \cdot n_s = -\frac{i\omega S_i}{|\nabla S|} + (\nabla\phi_\infty + \nabla\phi_s) \cdot n_i \tag{16}$$

$$C_{pu} = -\frac{2\alpha_0 e^{i\omega t}}{V_\infty^2}[(\nabla\phi_\infty + \nabla\phi_s) \cdot \nabla\phi_u + i\omega\psi] \tag{17}$$

$$\Delta\left[(\nabla\phi_\infty + \nabla\phi_s) \cdot \nabla\phi_u + \frac{\partial\phi_u}{\partial t}\right] = 0 \tag{18}$$

Since the wake is assumed to be the steady-state trailing-edge streamline, we can define ξ to be the coordinate parallel to the wake and write Eq. (18) as

$$\Delta\left[V_s(\xi)\frac{\partial\phi_u}{\partial\xi} + \frac{\partial\phi_u}{\partial t}\right] = 0 \tag{19}$$

Differentiating with respect to ξ and following the procedure outlined in Ref. 5, this expression results in

$$\frac{\partial}{\partial\xi}[V_s(\xi)\gamma(\xi,t)] + \frac{\partial}{\partial t}\gamma(\xi,t) = 0 \tag{20}$$

Now, in accordance with the definition of the unsteady velocity potential, letting

$$\gamma(\xi,t) = \bar{\gamma}(\xi)\alpha_0 e^{i\omega t} \tag{21}$$

and integrating from the trailing edge on along the wake,

$$\bar{\gamma}(\xi) = \frac{[\bar{\gamma}(\xi)V_s(\xi)]_{TE}}{V_s(\xi)} \exp\left[-i\omega\int_{TE}^{\xi}\frac{d\zeta}{V_s(\zeta)}\right] \tag{22}$$

where on the airfoil trailing edge

$$\bar{\gamma}(\xi)_{TE} = [\bar{\gamma}(\xi)^+ + \bar{\gamma}(\xi)^-]_{TE} \tag{23}$$

This expression gives the vorticity at any point along the wake in terms of the vorticity at the trailing edge and the steady-state velocity distribution along the wake, the latter quantity being known from the steady-state solution.

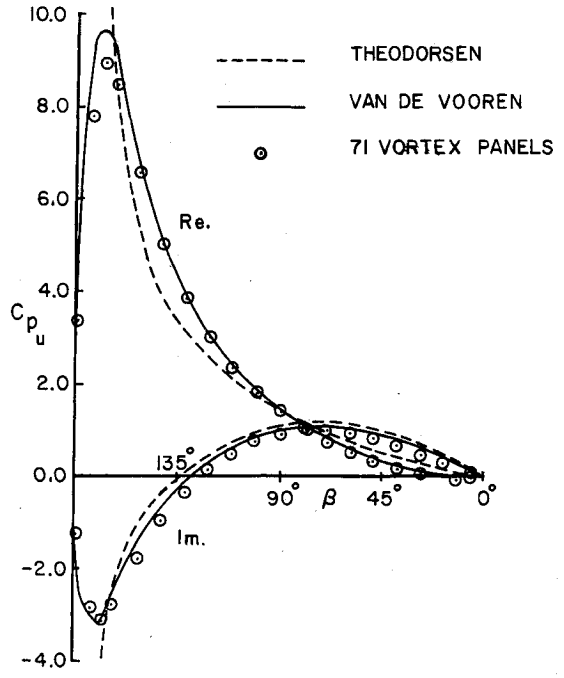

Fig. 1 Unsteady pressure distribution on the van de Vooren airfoil, $\bar{\omega} = 0.4$, $C/2$ torsion.

F. Discretization and Numerical Solution

The details of discretization and the numerical solution of the steady and the unsteady flow equations are presented in Ref. 16. However, a brief outline of the method will be presented here.

The formulation of the solution technique is in terms of the velocity potential. However, the actual solution process is carried out in terms of velocity. Since the flow equation is linear in both steady and unsteady flows, their solutions can be obtained using the superposition principle. Assuming that the surfaces of the airfoil and the wake are represented by continuous vortex sheets, the velocity potential at any field point (x,z) can be found from

$$2\pi\phi(x,z) = -\int_{\text{airfoil}} f_1(s)\theta \, ds - \int_{\text{wake}} f_2(s)\theta \, ds + \bar{C} \qquad (24)$$

where $f_1(s)$ and $f_2(s)$ represent distribution of vorticity on the airfoil and the wake surfaces, respectively. $\bar{C}$ is the constant of integration. Allowing (x,z) to be located on the surface and differentiating with respect to the steady-state normal to the surface

$$2\pi \nabla\phi(x,z)\cdot n_s = -\int_{\text{airfoil}} f_1(s)(\nabla\theta\cdot n_s)\, ds - \int_{\text{wake}} f_2(s)(\nabla\theta\cdot n_s)\, ds \qquad (25)$$

For the steady-state flow, $f_2(s)$ is identically zero because no vortices are shed into the wake, and the left side is known from the flow tangency condition. Therefore, Eq. (25) forms an integral equation with $f_1(s)$ as the unknown. This distribution can be found using the method of Ref. 18.

For the unsteady flow problem, the surfaces of the airfoil and the wake are divided into a finite number of straight line panels. A control point is placed at the center of each panel on the surface. These control points are used to satisfy the flow tangency condition. A vortex sheet with linear variation of vorticity $\bar{\gamma}_j(s)$ is placed on each panel while maintaining continuity of vorticity between adjacent panels. This results in the value of vorticity at every node being the unknown. As shown in Ref. 19, this is equivalent to using quadratically distributed doublets over each panel. Therefore, the velocity potential varies quadratically between every two neighboring nodes.

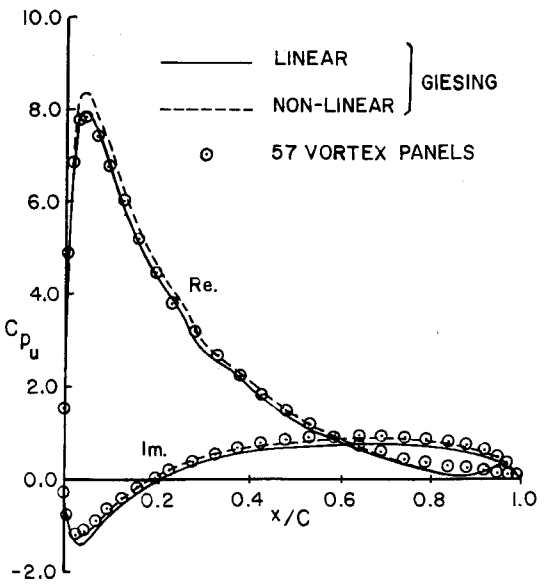

Fig. 2 Unsteady pressure distribution on a 25.5% Joukowski airfoil, $\bar{\omega}=\pi/10$, $C/4$ torsion.

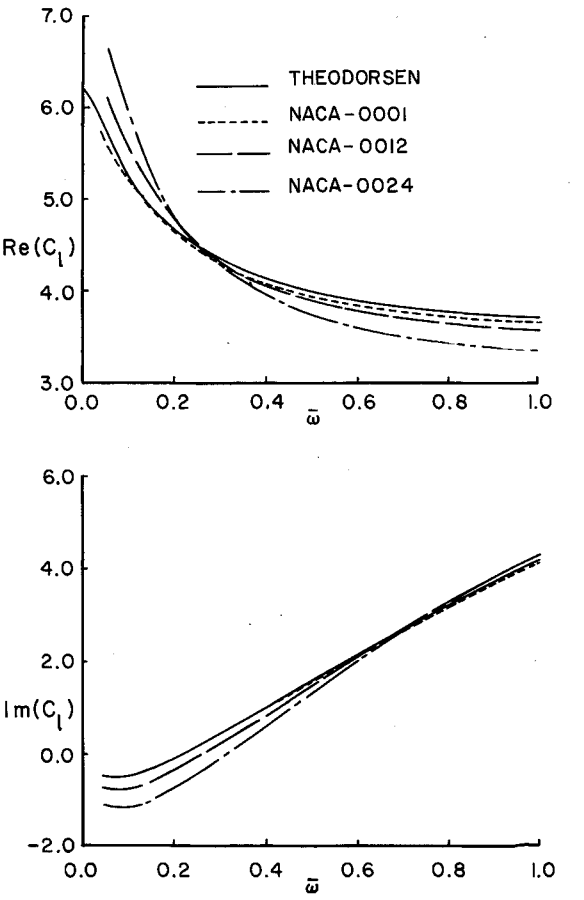

Fig. 3 Effect of thickness on unsteady lift coefficient of a single airfoil in pitch, $C/4$ torsion.

Assuming the airfoils are represented by N panels, Eq. (25) becomes

$$2\pi \nabla\psi(x,z)\cdot n_s = -\sum_{j=1}^{N}\int_{l_j} \bar{\gamma}_j(s)\nabla\theta\cdot n_s \, ds - \int_{TE}^{\infty} \bar{\gamma}(s)\nabla\theta\cdot n_s \, ds \qquad (26)$$

The left side of this equation is known at every control point from Eq. (16). On the right side, since $\bar{\gamma}_j(s)$ is assumed to be linear, the unknowns are the vortex strengths at the endpoints of the panels on the surface, the node points. In the wake integral, $\bar{\gamma}(s)$ is related to vorticity and velocity at the trailing-edge corners through Eqs. (22) and (23). Therefore, applying Eq. (26) to every panel will result in a set of linearly independent equations for the unknown vortices at the nodes. The integral of Eq. (22) can be performed using the simple trapezoidal rule. Near the trailing edge, where $V_s(\xi)$ varies very rapidly, step sizes of the order of 5% of the chord length have to be taken. Past a distance of approximately 10 chord lengths, the wake can be assumed flat with constant steady-state velocity, equal to that of the freestream. In this region, the integration step size can be increased to about 10% of the vorticity wave length. For complete convergence, it was determined that the semi-infinite integral of Eq. (26) had to be carried out to 150 chord lengths behind the trailing edge. Also, this model of the wake results in a closed-form solution for the total vorticity over that part of the wake. This total vorticity has to be fixed in order to satisfy the Kelvin's theorem or

$$\int_{\text{airfoil}} \bar{\gamma}(s)\, ds + \int_{\text{wake}} \bar{\gamma}(s)\, ds = \text{const} \qquad (27)$$

For convenience, this constant can be set to zero.

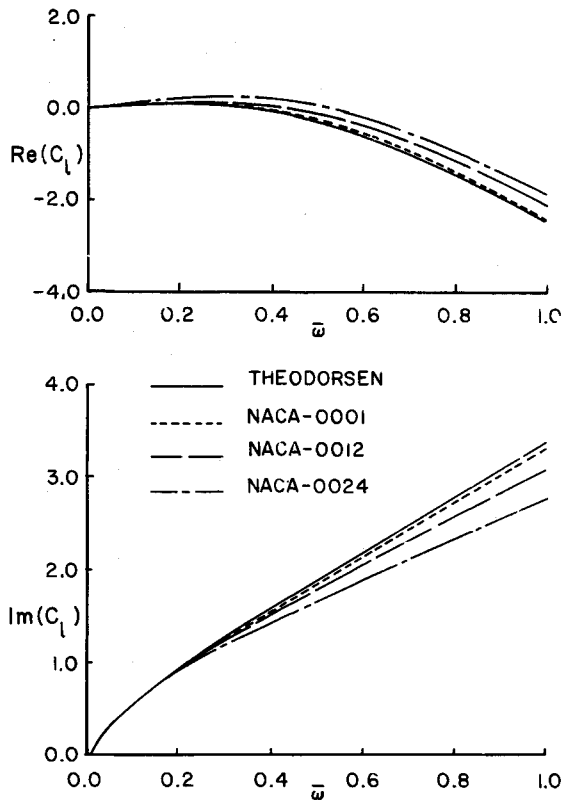

Fig. 4 Effect of thickness on unsteady lift coefficient of a single airfoil in plunge.

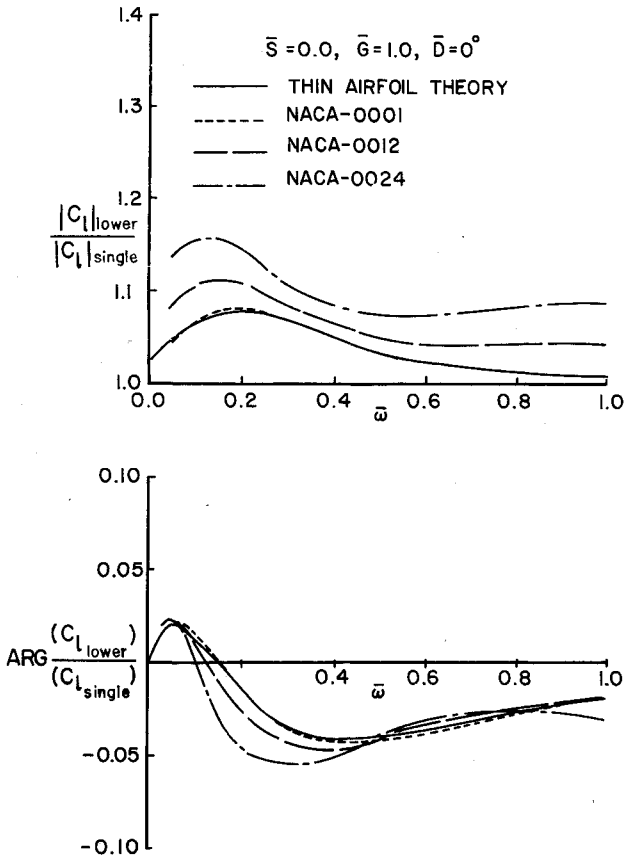

Fig. 5 Effect of thickness on lift coefficient of two parallel airfoils, stationary upper airfoil, plunging lower airfoil.

Once the unsteady vortex strengths are determined, the unsteady velocity distribution can be calculated from

$$2\pi \nabla\psi(x,z)\cdot \boldsymbol{e}_s = -\pi\bar{\gamma} - \sum_{j=1}^{N}\int_{l_j}\bar{\gamma}_j(s)\nabla\theta\cdot\boldsymbol{e}_s\,ds - \int_{TE}^{\infty}\bar{\gamma}(s)\nabla\theta\cdot\boldsymbol{e}_s\,ds \tag{28}$$

In order to find the unsteady velocity potential, the value of this parameter is assumed to be zero on one side of the trailing edge. Then a simple line integration of the velocity tangent to the surface results in the value of the velocity potential, unique to within a constant. For symmetric airfoils undergoing harmonic motion about a zero mean incidence angle, this constant can be determined from the pressure coefficient. In these cases, the pressure is an odd function with respect to the chord line. At the same time, from the Kutta condition, the difference between the upper and lower surface pressures must vanish at the trailing edge. This leads to the conclusion that, in such cases, the pressure coefficient itself must vanish at this point and allow exact calculation of this parameter everywhere over the surface.

III. Results and Discussion

A. Single Element Unsteady Solution

The first airfoil studied using this method was that of Ref. 5. Figure 1 shows the comparison of the pressure coefficient predicted analytically with that calculated using the vortex panel method. The airfoil is symmetric, approximately 14% thick, and has a finite trailing-edge angle. As demonstrated in this figure, excellent agreement between the two methods is

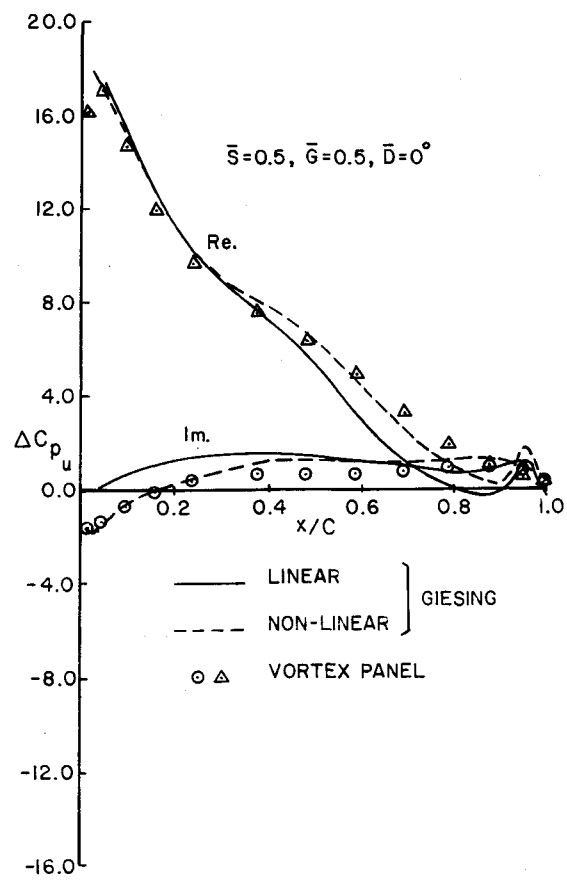

Fig. 6 Pressure distribution on pitching upper airfoil of two 25.5% thick Joukowski sections, stationary lower airfoil.

present everywhere except in the real part near the leading edge. The minor disagreements in this region are due to the lack of a sufficient number of points. In this case, due to the symmetry of the airfoil, the constant of integration for the velocity potential could be explicitly evaluated, resulting in the exact distribution of the pressure coefficient. Figure 2 shows the same type of comparison for a 25.5% thick Joukowski section, investigated in Refs. 8–10. The nonlinear data shown in this figure were extracted from Ref. 8 and were obtained using a time-marching technique. Again, there is excellent agreement among the three sets of results. However, a total absence of any oscillations in the pressure coefficient, as predicted by the vortex panel method, is clearly evident near the trailing edge. This is due to the greater accuracy of this method. The type of oscillation shown in this figure is quite typical of that obtained from source panel methods for airfoils with cusped trailing edges. In fact, in Refs. 8–10, the trailing-edge shape had to be modified in order to minimize these oscillations of the pressure coefficient. The 25.5% thick Joukowski airfoil was also used as the subject of a convergence test. The results for 49 panels differed from the results for 199 panels by a maximum of only 7% in the imaginary part of the lift coefficient.

Figures 3 and 4 show the effects of thickness on the lift coefficients over a wide range of reduced frequencies. The numerical results in these figures were all obtained with 71 vortex panels. Here, the trends are very much in agreement with those of Ref. 4. Also, as the reduced frequency decreases, the lift curve slope shown in Fig. 3 is seen to approach the steady-state potential value. Using conformal mapping, as shown in Ref. 20, these steady-state values are 6.33, 6.86, and 7.44 per rad for 1, 12, and 24% thick airfoils, respectively. In these figures, vortex panel results are also presented for an airfoil with a 1% thickness. The purpose of this exercise was

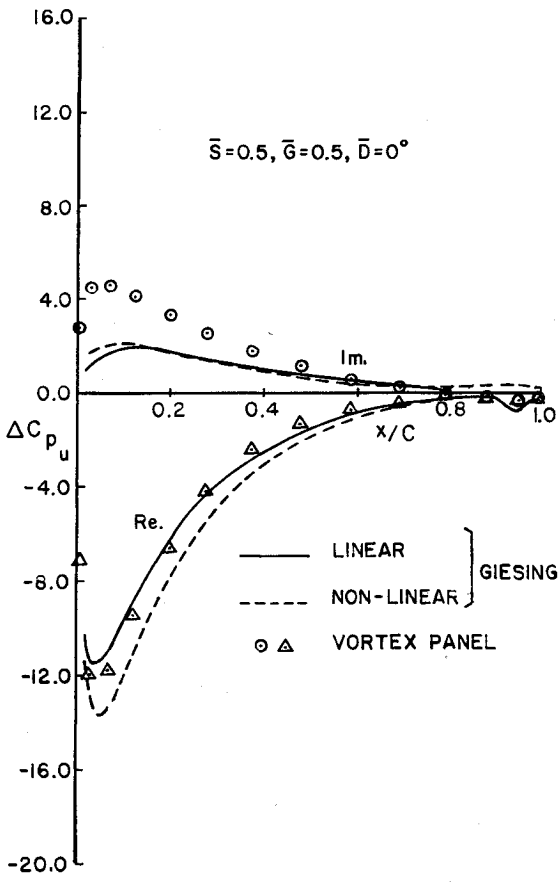

Fig. 7 Pressure distribution on stationary lower airfoil of two 25.5% thick Joukowski sections, pitching upper airfoil.

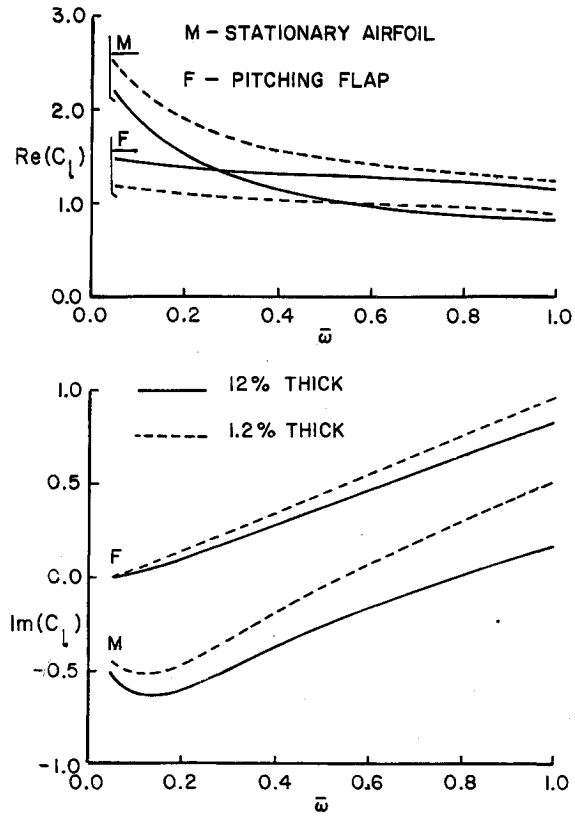

Fig. 8 Effect of thickness on lift coefficient of a NACA-23012 airfoil with a 30% chord slotted flap.

twofold. In the first place, it was intended to demonstrate the stability of the vortex panel method even for extremely small values of this parameter. Numerical schemes based on source panel techniques usually fail in such cases. Second, comparison of the aerodynamics coefficients for such an airfoil with those of the linear theory shows the ultimate convergence of the two methods as the thickness approaches zero. In addition, being assured of this fact, in considering multielement cases where analytical results are no longer available, would allow substitution of small thickness results instead.

B. Multielement Unsteady Solution

The lift coefficient predicted by the vortex panel method for two coupled airfoils was also compared with the results of Ref. 7. This comparison is shown in Fig. 5. In this case, two airfoils are used with a gap of one chord length, zero stagger, and zero decalage. Gap and stagger are defined as the vertical and horizontal separations of the airfoils, respectively. Positive stagger is associated with the top airfoil leading the lower airfoil, whereas gap is is defined to be always positive. Decalage angle is the relative inclination of the two airfoils, positive for the upper airfoil at a higher incidence angle than the lower airfoil. Here, the upper airfoil was stationary while the lower airfoil executed harmonic plunge. The solution in Ref. 7 relied on acceleration potential formulation, and the numerical scheme used there was considerably different. This figure shows the excellent agreement between the two methods for thickness ratio approaching zero. Also, it is quite evident from this figure that increasing thickness ratio results in stronger aerodynamic coupling between the airfoils. Logically, these effects were expected to magnify with increased aerodynamic coupling in the presence of smaller gaps or slotted flaps. These trends were in complete accordance with the steady-state solutions. Similar trends were also present in the values of the pitching moment coefficient except with slightly larger magnitude. Application of the results to a four-degree-of-freedom flutter model indicated flutter speeds of about

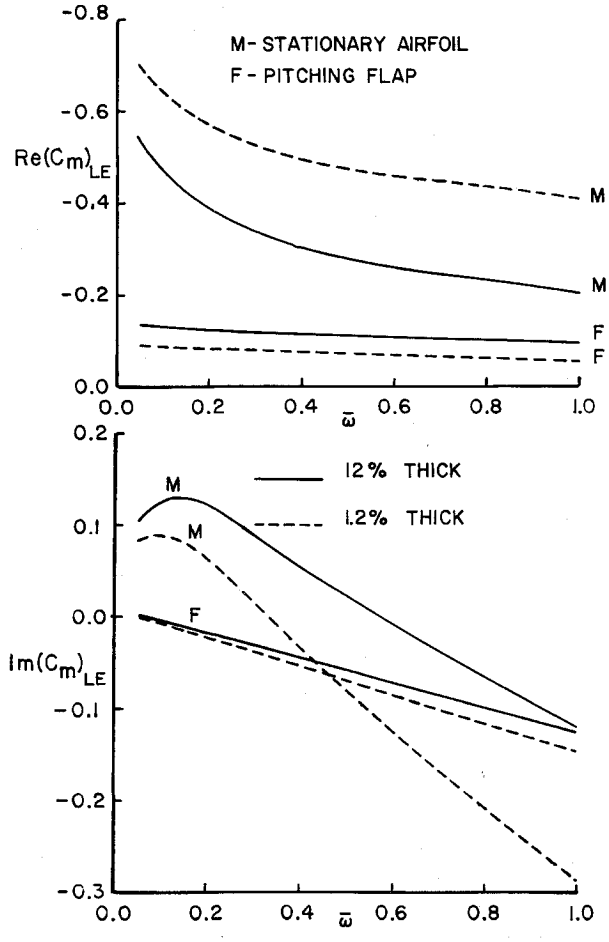

Fig. 9 Effect of thickness on pitching moment coefficient of a NACA-23012 airfoil with a 30% chord slotted flap.

10% lower for the 12% thick airfoils. The details of this analysis including the development and the solution of the equations of motion are presented in Ref. 16 and are beyond the scope of the current discussion.

Figures 6 and 7 show the comparison of results for two 25.5% thick Joukowski sections, with gap and stagger of one half chord length each. The lower airfoil was stationary with the upper airfoil in harmonic torsion about its quarter chord point. The linear solution was first presented in Ref. 8 and the nonlinear case was published in Ref. 10. Although these references contained the actual pressure coefficients, for the purpose of comparison with vortex panel results, they were converted to pressure differences. The good agreement among the three methods is quite evident in these figures. Also noticeable is the smooth pressure distribution near the trailing edges that is predicted by the vortex panel method. However, large discrepancies in the imaginary part of the pressure on the lower airfoil are quite apparent. At this point, the exact cause is unknown.

The final case considered here was that of a strongly coupled slotted flap. For this purpose, a NACA-23012 airfoil was fitted with a 30% chord slotted flap deflected to 20 deg and translated back by 5% of the chord. The main body of the airfoil was assumed stationary with the flap oscillating in torsion about its leading edge. It is noteworthy that this case cannot be modeled by any linear theory due to the large difference in the incidence angles of the airfoil and its flap. However, a model of the same geometry was constructed with the maximum thickness ratio reduced from 12 to 1.2%. Since the two models were identical in every respect, except for thickness ratio, any differences in pressures and aerodynamic forces had to be attributed to this parameter. The behavior of the lift and pitching moment coefficients over a wide range of frequencies is presented in Figs. 8 and 9. These figures show differences as large as 36% in the real part and 65% in the imaginary part of these parameters. These differences are present over the entire range of the reduced frequency and are certainly large enough to demonstrate the need for including the effects of thickness in these calculations. No flutter analysis was performed in this case, but based on the results obtained for the first case, thickness would be expected to reduce the flutter speed.

IV. Conclusions

Application of the vortex panel method was presented for solution of incompressible unsteady aerodynamic problems for lifting surfaces with finite thickness. The governing equation and the associated boundary conditions and constraints were developed for general unsteady flow. The equations were linearized for harmonic motion with small amplitude while maintaining the first-order effects of thickness. Integral equations for the solution of the resulting system of equations were presented. The accuracy and robustness of the method was demonstrated through comparisons with the existing numerical data and independent test cases. Also, through numerous examples, the flexibility of this method was shown in handling different types of geometries.

The vortex panel method was used to study the effects of airfoil thickness on aerodynamic coefficients of multielement lifting systems. It was demonstrated that, for single element airfoils, the effect of thickness is negligible and thin airfoil theory can be used with very good accuracy. However, it was shown that, for multiple lifting surfaces, thickness tends to magnify the interference effects. This was shown to have a profound effect on the aerodynamic coefficients vs those predicted by the thin airfoil theory. The difference in magnitudes and the phase angles predicted by the two approaches was shown to be large enough to warrant the inclusion of thickness in flutter calculations.

References

[1]Rokhsaz, K., "Aerodynamic Study of Dual Lifting Surfaces," M. S. Thesis, University of Missouri-Rolla, Rolla, MO, 1980.

[2]Rokhsaz, K., and Selberg, B. P., "Disadvantages of Thin Airfoil Formulations for Closely Coupled Airfoils," *Journal of Aircraft*, Vol. 20, No. 6, 1980, pp. 574-576.

[3]Theodorsen, T., "General Theory of Aerodynamic Instability and the Mechanism of Flutter," NACA Rept. 496, May 1934.

[4]Hewsone-Browne, R. C., "The Oscillation of a Thick Airfoil in an Incompressible Flow," *Quarterly Journal of Mechanics and Applied Mathematics*, Vol. 16, Pt. 1, 1963, pp. 79-92.

[5]Van de Vooren, A. I., and van de Vel, H., "Unsteady Profile Theory in Incompressible Flow," *Archiwum Mechaniki Stosowanej*, Vol. 3, No. 16, 1963, pp. 709-735.

[6]Possio, C., "L'Azione Aerodynamica sul Profilo Oscillante in un Fluido Compressible a Velocita Isoponara," *L'Aerodynamics*, Vol. 18, No. 4, 1938, pp. 441-458.

[7]Grzedzinski, J., "Aerodynamic Interference in a System of Two Harmonically Oscillating Airfoils in an Incompressible Flow," *Archiwum Mechaniki Stosowanej*, Vol. 26, No. 3, 1974, pp. 383-389.

[8]Giesing, J. P., "Nonlinear Two-Dimensional Unsteady Potential Flow with Lift," *Journal of Aircraft*, Vol. 5, No. 2, 1968, pp. 135-143.

[9]Giesing, J. P., "Nonlinear Interaction of Two Lifting Bodies in Arbitrary Unsteady Motion," *Journal of Basic Engineering*, Vol. 90, Series D, No. 3, 1968, pp. 387-394.

[10]Giesing, J. P., "Two-Dimensional Potential Flow Theory for Multiple Bodies in Small Amplitude Motion," *AIAA Journal*, Vol. 8, No. 11, 1968, pp. 1944-1953.

[11]Hess, J. L., "The Problem of 3-D Lifting Potential Flow and Its Solution by Means of Surface Singularity Distributions," *Computer Methods in Applied Mechanics and Engineering*, Vol. 4, No. 3, 1974, pp. 283-319.

[12]Hess, J. L., "The Use of Higher-Order Surface Singularity Distributions to Obtain Improved Potential Flow Solutions for Two-Dimensional Lifting Airfoils," *Computer Methods in Applied Mechanics and Engineering*, Vol. 5, No. 1, 1975, pp. 11-35.

[13]Hounjet, M. H. L., "ARSPNSC: A Method to Calculate Sub-

sonic Steady and Unsteady Potential Flow About Complex Configurations," National Aerospace Lab., Amsterdam, The Netherlands, TR-86122-U, Dec. 1986.

[14]Morino, L., "Steady, Oscillatory, and Unsteady Subsonic and Supersonic Aerodynamics—Production Version (SOUSSA-P 1.1)—Volume I—Theoretical Manual," NASA CR-NAS1-14977, Jan. 1980.

[15]Banerjee, P. K., and Butterfield, R., *Boundary Element Methods in Engineering Science*, McGraw-Hill, United Kingdom, 1981.

[16]Rokhsaz, K., "A Vortex Panel Method for Unsteady Aerodynamics of Multiple Lifting Surfaces with Thickness," Ph.D. Dissertation, University of Missouri-Rolla, Rolla, MO, 1988.

[17]Kuethe, A. M., and Chow, C. Y., *Foundations of Aerodynamics*, 4th ed., Wiley, New York, 1986.

[18]Stevens, W. A., Goradia, S. H., and Braden, J. A., "Mathematical Model for Two-Dimensional Multi-Component Airfoils in Viscous Flow," NASA CR-1843, July 1971.

[19]Moran, J., *An Introduction to Theoretical and Computational Aerodynamics*, Wiley, New York, 1984.

[20]Abbot, I. H., and von Doenhoff, A. E., *Theory of Wing Sections*, Dover, New York, 1959.